ACS APPLIED MATERIALS & INTERFACES

Research Article

www.acsami.org

Polydopamine-Coated Magnetic Nanoparticles for Enrichment and Direct Detection of Small Molecule Pollutants Coupled with MALDI-TOF-MS

Yu-rong Ma,[†] Xiao-le Zhang,[†,‡] Tao Zeng,[†] Dong Cao,[†] Zhen Zhou,[†] Wen-hui Li,[†] Hongyun Niu,[†] and Ya-qi Cai*[,†]

[†]The State Key Laboratory of Environmental Chemistry and Ecotoxicology of the Research Center for Eco-Environmental Sciences, Chinese Academy of Sciences, Beijing 100085, China

[‡]College of Life Science, Hebei United University, Tangshan, Hebei, 063000, China

Supporting Information

ABSTRACT: Polydopamine-coated Fe_3O_4 nanoparticles (Fe_3O_4@PDA NPs) were synthesized and applied as matrix for the detection of pollutants by matrix-assisted laser desorption/ionization time-of-flight mass spectrometry (MALDI-TOF-MS). The synthesis of Fe_3O_4@PDA NPs was accomplished in 30 min by in situ polymerization of dopamine without any toxic reagent. Using Fe_3O_4@PDA NPs as matrix of MALDI-TOF, eleven small molecule pollutants (molecular weight from 251.6 to 499.3), including Benzo(a)pyrene (BaP), three perfluorinated compounds (PFCs), and seven antibiotics, were successfully detected in either positive or negative reflection mode without background interference. Furthermore, the Fe_3O_4@PDA NPs can also enrich trace amounts of hydrophobic target, such as BaP, from solution to nanoparticles surface. Then the Fe_3O_4@PDA-BaP can be isolated through magnetic sedimentation step and directly spotted on the stainless steel plate for MALDI measurement. With Fe_3O_4@PDA NPs as adsorbent and matrix, we also realized the analysis of BaP in tap water and lake water samples. Thus, a magnetic solid-phase extraction (MSPE)-MALDI-TOF-MS method was established for the measurement of BaP.

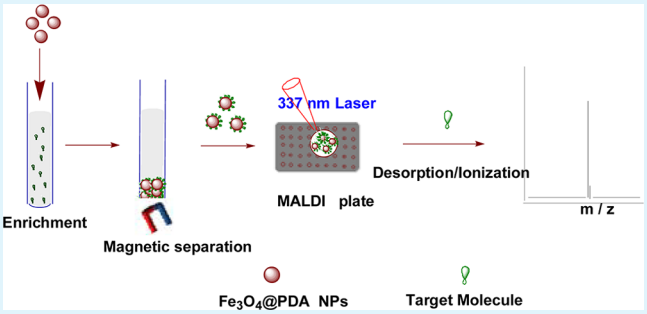

KEYWORDS: *matrix-assisted laser desorption/ionization time-of-flight mass spectrometry, polydopamine, Fe_3O_4 nanoparticles, benzo(a)pyrene, matrix*

INTRODUCTION

Matrix-assisted laser desorption/ionization (MALDI) has received great development since its appearing in the later 1980s.[1] In contrast to the conventional techniques such as liquid chromatography tandem triple quadrupole mass spectrometry(LC-MS/MS), gas chromatography mass spectrometry (GC-MS), and high-performance liquid chromatography with fluorescence detector (HPLC-FLD), MALDI analysis have the advantages of short-time experimental cycle, simple pretreatment procedure, and low consumption of samples.[2−6] However, according to previous report, MALDI-TOF-MS are mainly focused on the analysis of peptides and proteins in biological field rather than environmental pollutants.[7−12] Because traditional organic matrix produces intense signal interference toward the targets less than 500 Da, which greatly limits the application of MALDI in the measurement of small molecules.[13] To solve the matrix-related background interference problem, scientists have developed surfactant-suppressed and nanomaterial matrix.[6,13] Nanomaterials, especially metal nanoparticles (NPs) and carbon nanomaterials, can largely absorb laser energy and transfer the energy to target molecule, which facilitates the desorption and ionization of target molecule.[14−17] Compared to traditional matrix, nanomaterials generate little background signal of less than 500 Da and widen the application field of MALDI into the detection of small molecules.[18−20] With the rapid development of nanomaterial chemistry, graphene, Fe_3O_4@matrix, Au@SiO_2, Au NPs, and graphene@multiwalled carbon nanotube have already been employed as matrix for testing spermine,[4] salicylamide,[18] mefenamic acid,[18] small functional molecules,[21] glucose,[22] amino acids,[23] et al.

To improve the detection sensitivity and the anti-interference ability to the impurity substances contained in samples or introduced during the pretreatment process, an enrichment and purification procedure is always necessary to extract target molecule from complicate system before MALDI measurement.[24,25] Polymer-coated metal nanoparticles and carbon nanomaterials, with large surface area and π-conjugated

Received: November 14, 2012
Accepted: January 9, 2013
Published: January 9, 2013

Scheme 1. Procedure of MALDI-TOF-MS Based on Fe_3O_4@PDA NPs as Adsorbent and Matrix

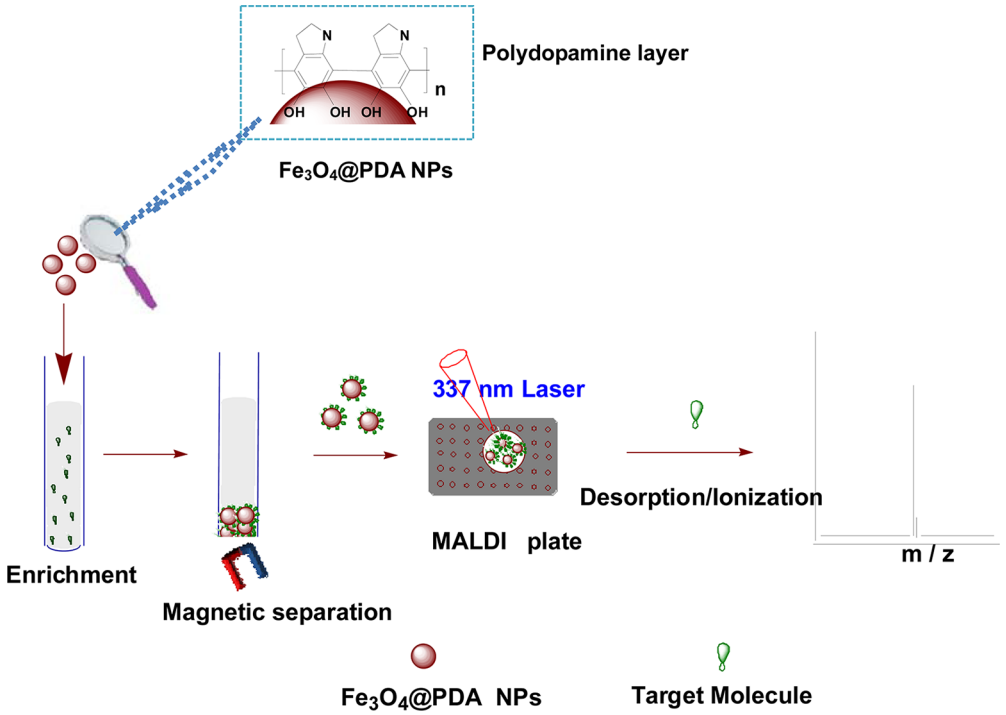

networks, show high affinity toward hydrophobic molecules and have been used as effective affinity probes and matrix in MALDI technique.[4,26] However, the centrifugation step for the isolation of the affinity probes is time-consuming and would greatly complicate the experimental procedure.[10] Furthermore it is impossible to thoroughly retrieve the analyte-adsorbed material from solution even by centrifugation at high speed, which would cause sample loss during separation step and limit the determination of trace analytes.[24] Magnetic nanoparticles (MNPs), with unique magnetic separation ability, can simplify the isolation procedure and speed up the assay process.[18,27] Recently, carbon materials functionalized MNPs, such as MNPs-graphene-TiO2, MNPs@carbon@TiO2, and MNPs@C8, have been constructed as adsorbent for peptides and proteins which still require the involvement of organic matrix during the MALDI measurement.[17,28,29] MNPs@graphene and MNPs@carbon nanotube can be utilized as both adsorbent and matrix for small molecules with MALDI-TOF-MS.[19,24] However, the acquisition of functionalized MNPs usually needs multiple manipulations, high temperature management and long-time experimental cycle from 24 h to several days, which is laborious and time-consuming. Therefore, a facile and fast MNP-based adsorbent and matrix are urgent to be developed for MALDI measurement.

Dopamine, a constituent acting crucial roles in neuro signal transmission and study-memory activity, has attracted substantial interest in various scientific fields for its excellent chemical property.[30,31] It can self-polymerize in alkaline solution and the generated polydopamine could adhere onto almost all the organic and inorganic surfaces including noble metals, metal oxides, polymers and ceramics.[30] Inspired by the unique property of dopamine, polydopamine-coated Fe_3O_4 (Fe_3O_4@PDA) NPs were constructed by in situ polymerization of dopamine on Fe_3O_4 surface in this research. Furthermore, the unique structure and active groups of the polydopamine coating also endows the Fe_3O_4@PDA NPs with high performance as MALDI matrix. Hence, the Fe_3O_4@PDA NPs may serve as matrix in the MALDI-TOF-MS analysis of small molecules. Benzo(a)pyrene (BaP), one of polycyclic aromatic hydrocarbons (PAHs) with high toxic and carcinogenic properties,[3] was chosen to investigate the matrix function of Fe_3O_4@PDA NPs with MALDI measurement in positive reflection mode. Three perfluorinated compounds (PFCs, a group of persistent organic compounds)[27] and seven antibiotics (widely used with undesirable effects on ecosystems and humans)[2] were selected to investigate the performance of Fe_3O_4@PDA NPs as MALDI matrix in negative reflection mode. Relying on the $\pi-\pi$ structure of polydopamine, there are strong analyte related mass spectrum signal in either positive or negative mode for MALDI measurement. According to previous report, the polydopamine coat, cross-linked by C−C bond, has excellent enrichment ability to hydrophobic molecules because of the $\pi-\pi$ bonds in the nanostructure.[30,32−34] Combining with the magnetic property of Fe_3O_4 core and the high affinity and matrix effect of polydopamine shell, the Fe_3O_4@PDA NPs can be utilized as solid phase extraction (SPE) adsorbent for trace BaP and isolated through magnetic sedimentation step and directly dotted for MALDI measurement (Scheme 1). The proposed strategy provides a simple, fast, and sensitive way for analyzing environmental pollutants with MALDI-TOF-MS technique.

EXPERIMENTAL SECTION

Chemicals. The 3-hydroxytyramine hydrochloride (dopamine) and Tri(hydroxymethyl)-aminomethane(Tris) were purchased from J&K Chemical Ltd. (China). Ferrous chloride tetrahydrate ($FeCl_2{\cdot}4H_2O$), ferric trichloride hexahydrate ($FeCl_3{\cdot}6H_2O$) were from Sinopharm Chemical Reagent Co., Ltd., (Shanghai, China). Benzo(a)pyrene (BaP) was obtained from AccuStandard (New Haven, USA) and dissolved in acetonitrile for use. Perfluorobutyric sulfonate (PFBS), perfluorohexane sulfonate (PFHxS) and perfluorooctanic sulfonate (PFOS) were obtained from Sigma-Aldrich and were dissolved in ultrapure water to acquired concentration. Norfloxacin (NOR),

dx.doi.org/10.1021/am3027025 | ACS Appl. Mater. Interfaces 2013, 5, 1024−1030

ciprofloxacin (CIP), difloxacin (DIF), enrofloxacin (ENR), fleroxacin (FLE), lomefloxacin (LOM), and sarafloxacin (SAR) were purchased from KaSei Industry Co., Ltd. (Tokyo, Japan) and 50 mg L^{-1} of each antibiotic solution were prepared in methanol for use. Humic acid (HA) and bovine serum albumin (BSA) were supplied by Sigma–Aldrich (Steinheim, Germany). Acetonitrile and other chemicals were at least analytical grade and used as received. Ultrapure water was prepared by using a Milli-Q water purification system (Millipore, Bedford, MA, USA).

Instrument. Transmission electron microscope (TEM) studies were carried out with the H-7500 (Hitachi, Japan) operating at 80 kV accelerated voltage. X-ray photoelectron spectroscopy (XPS) measurements were performed with an ESCA-Lab-200i-XL spectrometer (Thermo Scientific, Waltham, MA) with monochromatic Al Kα radiation (1486.6 eV). FTIR spectra were conducted with a NEXUS 670 Infrared Fourier Transform Spectrometer (Nicolet Thermo, Waltham, MA). The magnetization curves of the products were measured with a vibrating sample magnetometer (VSM, LDJ9600, Troy, MI).

MALDI-TOF-MS Analysis. All mass spectra were obtained with an Autoflex III MALDI-TOF-MS (Bruker Daltonics, Germany). MALDI source was equipped with a nitrogen laser (337 nm) for irradiation of analytes and an accelerating voltage from −20 kV to 20 kV was employed. Mass spectra in both positive reflection mode and negative reflection mode were acquired with 200 laser shots with a LeCroy 9314 digital oscilloscope. All mass spectra were analyzed by Flex Analysis software provided by Bruker Daltonics Corp.

Preparation of Fe_3O_4@PDA NPs and MALDI-TOF Sample. First, Fe_3O_4 NPs were synthesized by the coprecipitation method[27] and redispersed in 200 mL of water for use after being washed twice each with ethanol and water. Next, the Fe_3O_4 NPs were coated with polydopamine. Briefly, 40 mL of the as-prepared Fe_3O_4 suspension, 242 mg of Tris, and 160 mL of water were added into a 250 mL conical flask, and the pH of the mixture was adjusted to 8.5 by 1 M HCl. Polydopamine coating was achieved by adding 400 mg of dopamine into the above solution under stirring and 20 mL of the reaction solution was taken out from the conical flask at required time to obtain Fe_3O_4@PDA NPs with different reaction time. The obtained Fe_3O_4@PDA NPs were washed with water for 5 times to remove the unreacted dopamine and dried at 50 °C for further MALDI-TOF-MS analysis.

Matrix solution was obtained by dispersing 1 mg of Fe_3O_4@PDA NPs in 3 mL of ultrapure water. The mixture of 5 μL of the above Fe_3O_4@PDA and 5 μL of analyte solution was vortexed for 40 s, followed by directly doting 1 μL of the matrix–analyte mixture onto the MALDI plate and dried in air for MALDI-TOF-MS analysis.

Enrichment and Analysis of BaP from Real Water Samples. MALDI measurement was introduced to detect the enrichment ability of the Fe_3O_4@PDA NPs. The procedure was as follows: 200 μg of the Fe_3O_4@PDA NPs was added into 10 mL of BaP water solution (1pg μL^{-1}), the mixture was then vortexed for 1 min and kept still for enrichment. After 30 min, the Fe_3O_4@PDA NPs were isolated with an external magnet and were redispersed in 500 μL of acetonitrile water solution (50%, V:V) and 1 μL of the above mixture was spotted directly onto the stainless steel plate for the MALDI analysis.

Lake water and tap water were filtered through 0.45 μm nylon filter. Ten microliters of 1 mg L^{-1} BaP standard solution was added into 10 mL of the real water samples and vortexed for 1 min. Next, 200 μg of Fe_3O_4@PDA NPs were added into the spiked-water sample for enrichment for 30 min. The Fe_3O_4@PDA NPs were then separated from the solution by external magnetic field and redispersed in a mixture of 500 μL of acetonitrile water solution (50%, V:V). The mixture (1 μL) was dotted on MALDI plate for MALDI-TOF-MS measurement.

RESULTS AND DISCUSSION

Characterization of Fe_3O_4@PDA NPs. The modification of Fe_3O_4 NPs with polydopamine was acquired by in situ polymerization of dopamine in tris-buffer solution (pH 8.5) with constant stirring. The successful generated Fe_3O_4@PDA nanostructure was further characterized by TEM, XPS, FTIR and VSM.

TEM measurement was used to confirm the nanostructure of Fe_3O_4@PDA NPs. As shown in Figure 1A, the as prepared

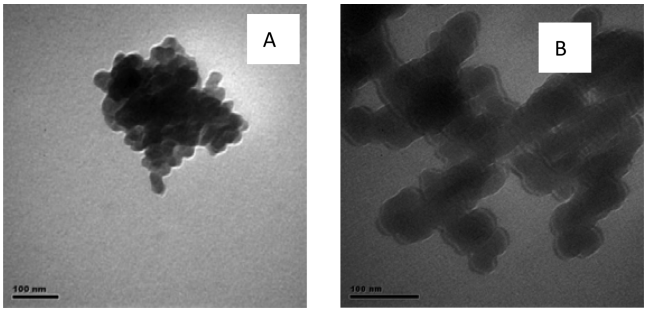

Figure 1. TEM images of (A) Fe_3O_4 NPs and (B) Fe_3O_4@PDA NPs.

Fe_3O_4 NPs are 28 nm in diameter. TEM images in Figure 1B suggest the formation of a polymer layer of 10 nm in thickness after 24 h of modification procedure. The generated polydopamine would be tightly coated onto the surface of Fe_3O_4 NPs through the catechol groups of dopamine.

XPS spectrum further testified the successful coating of polydopamine on Fe_3O_4 NPs. Fe_3O_4 NPs alone shows strong Fe2p signal (Figure 2). After the dopamine modification, N1s

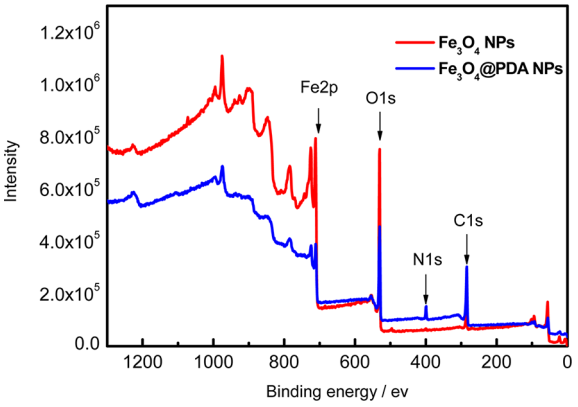

Figure 2. XPS spectrum of Fe_3O_4 NPs and Fe_3O_4@PDA NPs.

peak signal appears and the C1s peak signal obviously increases, which suggests the appearance of polydopamine on Fe_3O_4 NPs.[35] At the same time, the polydopamine coating of the nanostructure also induces the decreasing intensity of Fe2p peak.

FTIR spectrum measurement obtained the similar results. As shown in Figure 3, the absorption bands at 1290, 1486, 1614, and 3450 cm^{-1} can all be ascribed to the functional groups of dopamine.[36] The bands intensity at 1290 and 1486 cm^{-1} appear in the FTIR spectra of Fe_3O_4@PDA NPs and increase with the increasing dopamine modification time, indicating the increasing thickness of polydopamine layer.

VSM measurement was employed to investigate the magnetic properties of the nanostructure. As shown in Figure 4, the saturation magnetization of the nanostructure decreases with the increasing time of dopamine modification. This phenomenon can be explained by the increasing thickness of the nonmagnetic polydopamine layer. After 24 h of

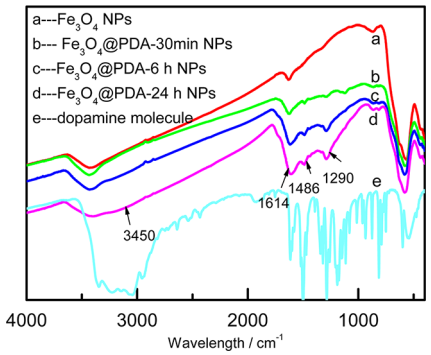

Figure 3. FTIR spectrum of free dopamine molecule, Fe_3O_4 NPs, Fe_3O_4@PDA NPs with different dopamine modification time.

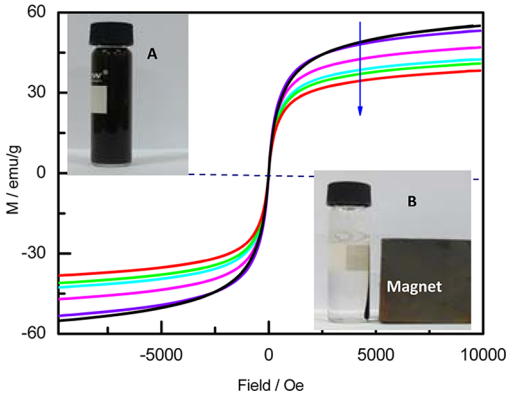

Figure 4. VSM magnetization curves of corresponding nanoparticles, from upper to lower: Fe_3O_4, Fe_3O_4@PDA-30 min, Fe_3O_4@PDA-2h, Fe_3O_4@PDA-4h, Fe_3O_4@PDA-6h and Fe_3O_4@PDA-24h. Inset shows the photographs of Fe_3O_4@PDA-24h NPs solution (A) before and (B) after magnetic separation.

modification, the saturation magnetization of the Fe_3O_4@PDA NPs can reach 37 emu g^{-1}, which is still sufficient for the magnetic separation.

Application of Fe_3O_4@PDA NPs as Matrix in MALDI-TOF-MS. As shown in the UV–vis spectrum of Figure S1 in the Supporting Information, polydopamine have absorption around 337 nm, which makes it absorb laser energy and transfer energy to analyte possible.[37] The acquisition of polydopamine could be achieved by in situ polymerization of dopamine without any toxic reagent. $\pi-\pi$ stacking structure, −OH group, electron-deficient quinone structure and amine group, all make polydopamine a proton and electron donor or acceptor, which facilitates Fe3O4@PDA as matrix in MALDI-TOF-MS technique.[32,38] The absorption of laser energy of 337 nm, easy-to-acquisition and functional groups of polydopamine all make polydopamine a potential and promise matrix for MALDI analysis.

Taking Fe_3O_4@PDA NPs as matrix and BaP as model molecule, we carried out a MALDI-TOF-MS study to investigate the matrix assistant function of the proposed nanostructure. The mass spectrum of BaP is shown in Figure 5. There is no $[BaP\text{-}e^-]^+$ signal detected at 251.6 when using Fe_3O_4 NPs as matrix. But with Fe_3O_4@PDA NPs as matrix, the mass spectrum at 251.6 $[BaP\text{-}e^-]^+$ appeared and sharply increased to about 650 au. The involvement of polydopamine in the nanostructure makes the determination of BaP by MALDI technique possible with no background signal interference. The high signal response can be attributed to

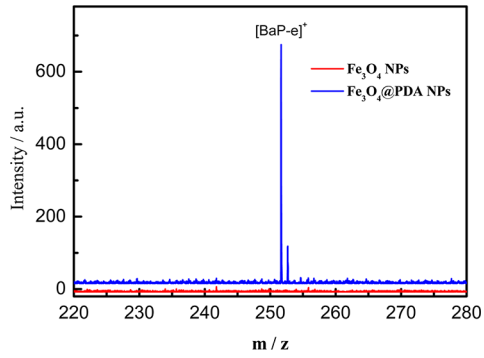

Figure 5. MALDI mass spectrum of 50 pg of BaP in positive reflection mode with Fe_3O_4 NPs and Fe_3O_4@PDA NPs as matrix.

two main reasons. First, because of the hydrophobic interaction between polydopamine and the benzene rings of the target, polydopamine layer could capture BaP from solution to the surface of the nanostructure, which facilitates the desorption/ionization of BaP. Second, $\pi-\pi$ stacking structure of polydopamine is helpful for the laser energy absorption and the transference of the energy to BaP.[4] Traditional matrix, including cyano-4-hydroxycinnamicacid (CHCA), 2, 5-dihydroxybenzoic acid (2, 5-DHB) and sinapic acid (SA), were also employed for the MALDI-TOF measurement of BaP and the results are presented in Figure S2 in the Supporting Information. As noted from the mass spectrum, BaP ion signal can be detected using CHCA and DHB as matrix but with strong background interference and there was no BaP ion signal when SA was utilized as matrix. Therefore, the Fe_3O_4@PDA NPs are more suitable for the MALDI-TOF-MS analysis of BaP than the traditional matrix.

To obtain the best mass signal response, we optimized the matrix amount and dopamine modification time. The mass spectrum of BaP with different concentrations of matrix is presented in Figure S3A in the Supporting Information. Every matrix concentration was measured by two parallel groups and each group was collected at least four measurements. The error bar in Figure S3A in the Supporting Information is given by eight measurements. As shown in Figure S3A in the Supporting Information, the peak intensity of BaP increased with the increasing amount of matrix from 0.10 to 0.33 $\mu g\ \mu L^{-1}$ but decreased dramatically from 0.33 to 5.0 $\mu g\ \mu L^{-1}$. This can be explained by the decreased energy transfer efficiency at high concentration of matrix. Therefore, the optimal matrix concentration for BaP in MALDI is 0.33 $\mu g\ \mu L^{-1}$. The effect of the dopamine modification time on the MALDI performance is displayed in Figure S3B in the Supporting Information. We found that the BaP signal response decreased with the increasing modification time (from 30 min to 24 h). Dopamine modification time determines the polydopamine layer thickness, thus affects the MALDI performance. Thicker polydopamine layer have stronger affinity toward BaP and too strong adsorption would hinder the desorption/ionization of BaP.[21] Finally, 30 min was chosen as the modification time for the constructing of Fe_3O_4@PDA NPs. Different concentrations of BaP were employed to examine the sensitivity of the Fe_3O_4@PDA NPs as matrix with the optimized condition for MALDI. As shown in Figure 6, BaP could even be detected at 5 pg and no apparent background noise existed in the mass spectrum. In addition, the BaP peak intensity increased obviously with the increasing BaP concentration. As a result, Fe_3O_4@PDA NPs is

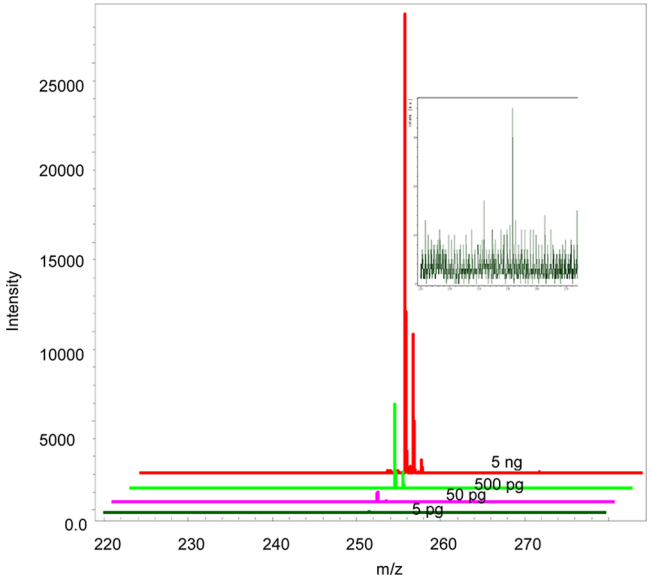

Figure 6. MALDI mass spectrum of different amount of BaP in positive mode with Fe_3O_4@PDA NPs as matrix. Inset shows the original mass spectrum of 5pg BaP.

possible to be utilized as matrix for the measurement of BaP with MALDI technique.

Except for the positive ionization mode, negative desorption/ionization mode is also a common mode for the studying of small molecules. Three PFCs and seven antibiotics were used to confirm the application of Fe_3O_4@PDA NPs as matrix in negative reflection mode with MALDI. Using CHCA and DHB as matrix, the mass spectrum of PFOS showed strong matrix ion interferences (data not shown). But when Fe_3O_4@PDA NPs were used as matrix, the sulfonic group of PFOS was easy to be deprotonated into $[PFOS\text{-}H]^-$ which could be detected in the negative reflection mode at 499.3 (Figure 7). Similarly, the signal of $[PFBS\text{-}H]^-$ and $[PFHxS\text{-}H]^-$ could be detected at 299.5 and 399.5 without matrix interferences (see Figure S4 in the Supporting Information). The sensitivity of PFBS, and

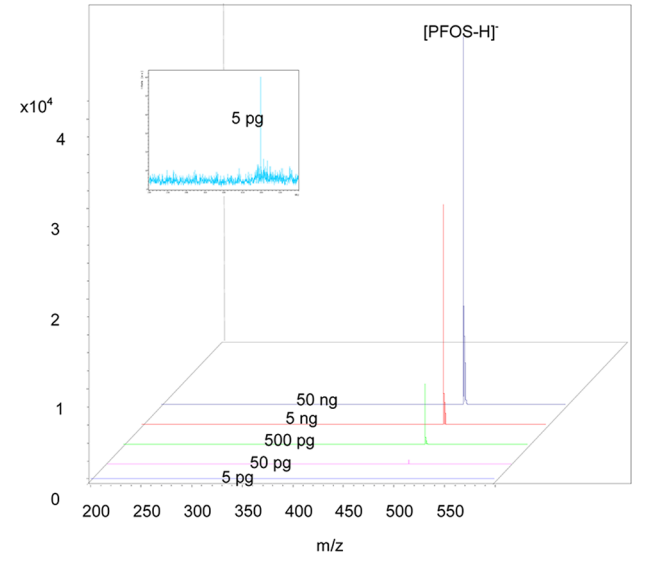

Figure 7. MALDI-TOF mass spectrum of different amount of PFOS with Fe_3O_4@PDA NPs as matrix in negative reflection mode. Inset shows the original mass spectrum of 5 pg PFOS.

PFHxS were also examined with MALDI measurement and the detection limit could reach 5 pg for each. Using Fe_3O_4@PDA NPs as matrix, seven antibiotic drugs were also measured by MALDI technique and the results are list in Figure S5 in the Supporting Information. From the structure and the mass spectrum of antibiotics, we could conclude that the N−C bond is prone to be broken up by the laser energy and the left negative ions could all be detected with MALDI measurement.

To further prove the analytical performance of Fe_3O_4@PDA NPs as matrix, we applied Fe_3O_4@PDA NPs for the analysis of a mixture of BaP, three PFCs, and seven antibiotics. As shown in Figure S6 in the Supporting Information, BaP, three PFCs, DIF, and ENR were all detected in their ionized fragment. However, it is still difficult to distinguish SAR, NOR, and CIP, because they have the same mass/charge ratio at 290, and both FLE and LOM have the same mass/charge ratio at 321. The functional group of matrix and analyte could affect the ionization efficiency with MALDI measurement. −OH group, electron-deficient quinone structure and $\pi-\pi$ stacking structure, make polydopamine a proton donor and an electron acceptor, which facilitates Fe_3O_4@PDA as matrix in positive mode.[37−39] BaP was chosen to test the matrix assistant function of Fe_3O_4@PDA as matrix in positive mode and BaP can be detected at 251.6 $[BaP\text{-}e^-]^+$. However, amine group and $\pi-\pi$ stacking structure also render polydopamine a proton acceptor, which favor Fe_3O_4@PDA as matrix in negative mode.[30,40] Three PFCs were chosen to study the matrix function of Fe_3O_4@PDA in negative mode and they were all detected in deprotonated form $[PFCs\text{-}H]^-$. Except for the property of matrix, functional group of the analyte also affect the ionization efficiency, so derivatization of small molecule is employed to improve the ionization efficiency with MALDI measurement.[41] While in this work, BaP is much more difficult to be ionized than three PFCs, because BaP do not contain any functional group while the acidic nature of PFCs make it easy to be deprotonated into $[PFCs\text{-}H]^-$, which means that the ionization efficiency in negative mode should be higher than in positive mode. However, there are more −OH groups and quinone structures than amine groups in polydopamine, which might make the ionization efficiency in positive mode higher than in the negative mode with Fe_3O_4@PDA as matrix. Therefore, it is difficult to compare the ionization efficiency in positive and negative mode in this work.

Fe_3O_4@PDA NPs as Adsorbent and Matrix for BaP. Considering the affinity interaction between polydopamine layer and the hydrophobic compounds,[34] Fe_3O_4@PDA NPs may serve as an adsorbent for analyte enrichment from solution. BaP, with five benzene rings, was chosen as model molecule to survey the enrichment ability of the nanostructure. The mass spectrum result is exhibited in Figure 8. The concentration of 1 pg μL^{-1} BaP is too low to be detected with MALDI. After 30 min of enrichment, there is an obvious BaP ion signal in MALDI spectrum, which indicated the high enrichment ability of Fe_3O_4@PDA NPs toward BaP. We further examined the effect of BaP concentration on the enrichment efficiency in Figure 9, and the BaP ion signal increased with the increasing amount of BaP.

Polydopamine-coated Fe_3O_4 also offers an adherent surface for natural organic matter and proteins, so we take humic acid (HA) and bovine serum albumin (BSA) as examples to investigate their interference toward BaP analysis with this method. Corresponding amount of HA or BSA was dispersed in 10 mL of Water containing 5 pg μL^{-1} BaP before enrichment

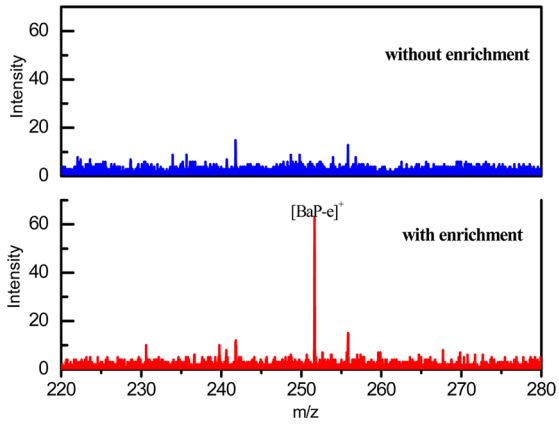

Figure 8. MALDI-TOF mass spectrum of 1 pg μL^{-1} BaP in pure water solution without and with Fe_3O_4@PDA NPs enrichment.

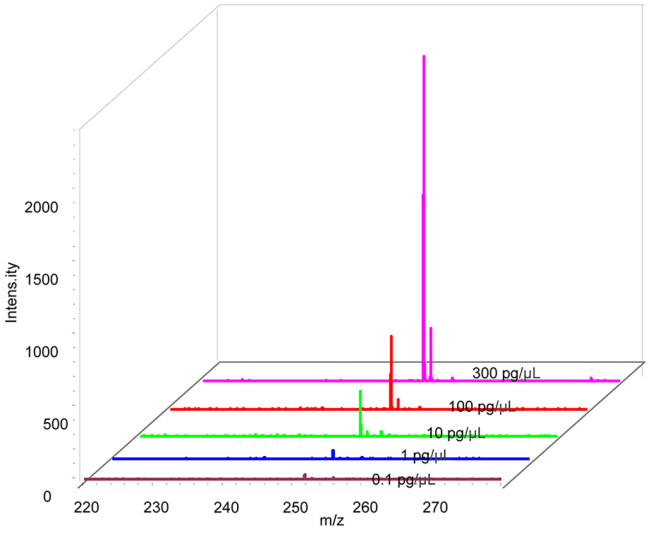

Figure 9. MALDI-TOF mass spectrum of different concentrations of BaP in water solution with Fe_3O_4@PDA NPs as adsorbent and matrix.

and the mixture went through the same enrichment procedure as the real water sample. As shown in Figure S7 in the Supporting Information, 5 mg L^{-1} BSA or HA did not interference the determination of BaP with Fe_3O_4@PDA NPs as adsorbent and matrix in this work. The amount of HA in water sample is about 1−5 mg L^{-1}, which means the coexistence of HA in water would not interfere the analysis of BaP in real water sample. Spiked experiments in real water samples were carried out to approve the application of the proposing strategy. There was a BaP ion signal in lake water and tap water with Fe_3O_4@PDA NPs as adsorbent and matrix (see Figure S8 in the Supporting Information). From the above results, we could speculate that the Fe_3O_4@PDA NPs have high enrichment performance to BaP and can be used as both adsorbent and matrix for MALDI measurement in real water sample.

CONCLUSIONS

In this article, Fe_3O_4@PDA NPs were prepared readily without the involvement of any toxic reagent. The obtained nanostructure can be utilized as MALDI matrix for measurement of small molecule pollutants in either positive or negative ion mode. In addition, the Fe_3O_4@PDA NPs show high affinity ability toward BaP. Therefore, they can be used as SPE adsorbent to enrich hydrophobic target efficiently from water solutions, isolated easily with a magnet, and directly spotted for MALDI analysis. Using Fe_3O_4@PDA NPs as both adsorbent and matrix, we realized the analysis of BaP in real water samples, and the results are satisfactory. This magnetic SPE-MALDI-TOF-MS measurement could be finished in 60 min, which largely improves the analysis efficiency. Fe_3O_4@PDA NPs show us a facile, high-speed, and environmentally friendly method to construct nanomaterial matrix and shows great promise in the environmental field.

ASSOCIATED CONTENT

Supporting Information

UV−vis spectrum of dopamine and polydopamine. MALDI mass spectrum of 50pg BaP in positive mode with CHCA, DHB, and SA as matrix. The effect of Fe_3O_4@PDA NPs matrix amount and dopamine modification time toward BaP MALDI signal response. MALDI-TOF mass spectrum of different amount of PFBS and PFHxS. MALDI-TOF mass spectrum of seven antibiotics. MALDI-MS spectrum of mixture of BaP, three PFCs and seven antibiotics. The effect of HA and BSA toward BaP analysis. detection of BaP in real water sample using Fe_3O_4@PDA NPs as absorbent and matrix. This material is available free of charge via the Internet at http://pubs.acs.org.

AUTHOR INFORMATION

Corresponding Author

*E-mail: caiyaqi@rcees.ac.cn. Tel: (086) 010-62849239. Fax: (086) 010-62849182.

Notes

The authors declare no competing financial interest.

ACKNOWLEDGMENTS

This work was jointly supported by the National Basic Research Program (Grants 2010CB933500) and the National Natural Science Foundation of China (Grants 20975110, 21277152, 21277002).

REFERENCES

(1) Karas, M.; Hillenkamp, F. *Anal. Chem.* **1988**, *60*, 2299−2301.
(2) Li, W.; Shi, Y.; Gao, L.; Liu, J.; Cai, Y. *Environ. Pollut.* **2012**, *162*, 56−62.
(3) Zhang, S.; Niu, H.; Zhang, Y.; Liu, J.; Shi, Y.; Zhang, X.; Cai, Y. *J. Chromatogr. A.* **2012**, *1238*, 38−45.
(4) Dong, X. L.; Cheng, J. S.; Li, J. H.; Wang, Y. S. *Anal. Chem.* **2010**, *82*, 6208−6214.
(5) Nicolaou, N.; Xu, Y.; Goodacre, R. *Anal. Chem.* **2012**, *84*, 5951−5958.
(6) Lu, M.; Lai, Y.; Chen, G.; Cai, Z. *Anal. Chem.* **2011**, *83*, 3161−3169.
(7) Lu, J.; Qi, D.; Deng, C.; Zhang, X.; Yang, P. *Nanoscale* **2010**, *2*, 1892−1900.
(8) Bechara, C.; Bolbach, G.; Bazzaco, P.; Sharma, K. S.; Durand, G.; Popot, J. L.; Zito, F.; Sagan, S. *Anal. Chem.* **2012**, *84*, 6128−6135.
(9) Anderson, D. S.; Heeney, M. M.; Roth, U.; Menzel, C.; Fleming, M. D.; Steen, H. *Anal. Chem.* **2010**, *82*, 1551−1555.
(10) Kong, X. L.; Huang, L. C. L.; Hsu, C. M.; Chen, W. H.; Han, C. C.; Chang, H. C. *Anal. Chem.* **2005**, *77*, 259−265.
(11) Persike, M.; Zimmermann, M.; Klein, J.; Karas, M. *Anal. Chem.* **2010**, *82*, 922−929.
(12) Zhou, X.; Wei, Y.; He, Q.; Boey, F.; Zhang, Q.; Zhang, H. *Chem. Commun.* **2010**, *46*, 6974−6976.

(13) Grant, D. C.; Helleur, R. J. *Rapid Commun. Mass Spectrom.* **2007**, *21*, 837−845.
(14) Gholipour, Y.; Giudicessi, S. L.; Nonami, H.; Erra-Balsells, R. *Anal. Chem.* **2010**, *82*, 5518−5526.
(15) Wang, K. Y.; Chuang, S. A.; Lin, P. C.; Huang, L. S.; Chen, S. H.; Ouarda, S.; Pan, W. H.; Lee, P. Y.; Lin, C. C.; Chen, Y. J. *Anal. Chem.* **2008**, *80*, 6159−6167.
(16) Jia, W.; Chen, X.; Lu, H.; Yang, P. *Angew. Chem., Int. Ed.* **2006**, *45*, 3345−3349.
(17) Min, Q.; Zhang, X.; Zhang, H.; Zhou, F.; Zhu, J. J. *Chem Commun.*. **2011**, *47*, 11709−11711.
(18) Lin, P. C.; Tseng, M. C.; Su, A. K.; Chen, Y. J.; Lin, C. C. *Anal. Chem.* **2007**, *79*, 3401−3408.
(19) Li, X. S.; Wu, J. H.; Xu, L. D.; Zhao, Q.; Luo, Y. B.; Yuan, B. F.; Feng, Y. Q. *Chem Commun.* **2011**, *47*, 9816−9818.
(20) Lorkiewicz, P.; Yappert, M. C. *Anal. Chem.* **2009**, *81*, 6596−6603.
(21) Zhu, X.; Wu, L.; Mungra, D. C.; Xia, S.; Zhu, J. *Analyst* **2012**, *137*, 2454−2458.
(22) Wu, H. P.; Yu, C. J.; Lin, C. Y.; Lin, Y. H.; Tseng, W. L. *J. Am. Soc. Mass Spectrom.* **2009**, *20*, 875−882.
(23) Kim, Y. K.; Na, H. K.; Kwack, S. J.; Ryoo, S. R.; Lee, Y.; Hong, S.; Hong, S.; Jeong, Y.; Min, D. H. *Acs Nano.* **2011**, *5*, 4550−4561.
(24) Shi, C.; Meng, J.; Deng, C. *Chem Commun.* **2012**, *48*, 2418−2420.
(25) Lu, J.; Wang, M.; Li, Y.; Deng, C. *Nanoscale* **2012**, *4*, 1577−1580.
(26) Shen, W. W.; Xiong, H. M.; Xu, Y.; Cai, S. J.; Lu, H. J.; Yang, P. Y. *Anal. Chem.* **2008**, *80*, 6758−6763.
(27) Zhang, X. L.; Niu, H. Y.; Pan, Y. Y.; Shi, Y. L.; Cai, Y. Q. *Anal. Chem.* **2010**, *82*, 2363−2371.
(28) Li, Y.; Wu, J.; Qi, D.; Xu, X.; Deng, C.; Yang, P.; Zhang, X. *Chem. Commun.* **2008**, 564−566.
(29) Chen, H.; Deng, C.; Li, Y.; Dai, Y.; Yang, P.; Zhang, X. *Adv. Mater.* **2009**, *21*, 2200−2205.
(30) Lee, H.; Dellatore, S. M.; Miller, W. M.; Messersmith, P. B. *Science* **2007**, *318*, 426−430.
(31) Ma, Y. R.; Niu, H. Y.; Zhang, X. L.; Cai, Y. Q. *Chem Commun.* **2011**, *47*, 12643−12645.
(32) Kong, J.; Yee, W. A.; Yang, L.; Wei, Y.; Phua, S. L.; Ong, H. G.; Ang, J. M.; Li, X.; Lu, X. *Chem Commun.* **2012**, *48*, 10316−10318.
(33) Lynge, M. E.; Ogaki, R.; Laursen, A. O.; Lovmand, J.; Sutherland, D. S.; Stadler, B. *ACS Appl Mater Interfaces* **2011**, *3*, 2142−2147.
(34) Morris, T. A.; Peterson, A. W.; Tarlov, M. J. *Anal. Chem.* **2009**, *81*, 5413−5420.
(35) Wei, Q.; Zhang, F.; Li, J.; Li, B.; Zhao, C. *Polym. Chem.* **2010**, *1*, 1430−1433.
(36) Fei, B.; Qian, B.; Yang, Z.; Wang, R.; Liu, W. C.; Mak, C. L.; Xin, J. H. *Carbon* **2008**, *46*, 1795−1797.
(37) Della Vecchia, N. F.; Avolio, R.; Alfè, M.; Errico, M. E.; Napolitano, A.; d'Ischia, M. *Adv. Funct. Mater.* **2012**, DOI: 10.1002/adfm.201202127.
(38) Chen, S.; Chen, L.; Wang, J.; Hou, J.; He, Q.; Liu, J.; Wang, J.; Xiong, S.; Yang, G.; Nie, Z. *Anal. Chem.* **2012**, *84*, 10291−10297.
(39) Pezzella, A.; Iadonisi, A.; Valerio, S.; Panzella, L.; Napolitano, A.; Adinolfi, M.; d'Ischia, M. *J. Am. Chem. Soc.* **2009**, *131*, 15270−15275.
(40) Cao, D.; Wang, Z.; Han, C.; Cui, L.; Hu, M.; Wu, J.; Liu, Y.; Cai, Y.; Wang, H.; Kang, Y. *Talanta* **2011**, *85*, 345−352.
(41) Gao, X.; Tang, Z.; Lu, M.; Liu, H.; Jiang, Y.; Zhao, Y.; Cai, Z. *Chem Commun.* **2012**, *48*, 10198−10200.